Characterization of humic acid reactivity modifications due to adsorption onto α-Al_2O_3

Noémie Janot, Pascal E. Reiller, X. Zheng, Jean-Philippe Croué, M.F. Benedetti

dx.doi.org/10.1016/j.watres.2011.11.042

Characterization of humic acid reactivity modifications due to adsorption onto α-Al_2O_3

Noémie Janot[a,b], Pascal E. Reiller[a], Xing Zheng[c], Jean-Philippe Croué[c], Marc F. Benedetti[b,]*

[a] Commissariat à l'Énergie Atomique, CE Saclay, CEA/DEN/DANS/DPC/SECR, Laboratoire de Spéciation des Radionucléides et des Molécules, Bâtiment 391 PC 33, Gif-sur-Yvette CEDEX, France.

[b] Univ. Paris Diderot, Sorbonne Paris Cité, Institut de Physique du Globe de Paris, UMR 7154 CNRS, Paris, France.

[c] King Abdullah University of Science and Technology Thuwal, Water Desalination and Reuse Research Center, Kingdom of Saudi Arabia.

* *Corresponding author*: benedetti@ipgp.fr

ABSTRACT

Adsorption of purified Aldrich humic acid (PAHA) onto α-Al_2O_3 is studied by batch experiments at different pH, ionic strength and coverage ratios R (mg of PAHA by m² of mineral surface). After equilibration, samples are centrifuged and the concentration of PAHA in the supernatants is measured. The amount of adsorbed PAHA per m² of mineral surface is decreasing with increasing pH. At constant pH value, the amount of adsorbed PAHA increases with initial PAHA concentration until pH-dependent a constant value is reached.

UV/Visible specific parameters such as specific absorbance $SUVA_{254}$, ratio of absorbance values E_2/E_3 and width of the electron-transfer absorbance band Δ_{ET} are calculated for supernatant PAHA fractions of adsorption experiments at pH 6.8, to have an insight on the evolution of PAHA characteristics with varying coverage ratio. No modification is observed compared to original compound for $R \geq 20$ mg_{PAHA}/g. Below this ratio, aromaticity decreases with initial PAHA concentration. Size-exclusion chromatography - organic carbon detection measurements on these supernatants also show a preferential adsorption of more aromatic and higher size fractions.

Spectrophotometric titrations were done to estimate changes of reactivity of supernatants from adsorption experiments made at $pH \approx 6.8$ and different PAHA concentrations. Evolutions of UV/Visible spectra with varying pH were treated to obtain titration curves that are interpreted within the NICA-Donnan framework. Protonation parameters of non-sorbed PAHA fractions are compared to those obtained for the PAHA before contact with the oxide. The amount of low-affinity type of sites and the value of their median affinity constant decrease after adsorption. From PAHA concentration in the supernatant and mass balance calculations, "titration curves" are obtained and fitted for the adsorbed fractions for the first time. These changes in reactivity to our opinion could explain the difficulty to model the behavior of ternary systems composed of pollutants/HS/mineral since additivity is not respected.

KEYWORDS

Adsorption; fractionation; DOC; mineral surface; organic matter

dx.doi.org/10.1016/j.watres.2011.11.042

1 Introduction

The interactions between humic substances (HS) and mineral surfaces modify their fate and their interactions with contaminants in the environment. Due to HS heterogeneous nature, their composition and binding properties are modified during adsorption onto minerals (Claret et al. 2008, Davis and Gloor 1981, Hur and Schlautman 2003, Janot et al. 2010, Reiller et al. 2006, Saito et al. 2004). Interactions between HS and mineral surfaces are controlled by different processes: electrostatic and hydrophobic interactions, ligand-exchange between phenolic and carboxylic groups of humic substances and mineral surface sites. The adsorption of humic substances onto mineral surfaces varies with pH, ionic strength, and concentration ratios between organic matter and minerals (Saito et al. 2004, Schlautman and Morgan 1994, Vermeer et al. 1998, Weng et al. 2007), but also with humic substances' origin and the type of mineral surface (Hur and Schlautman 2003).

During adsorption, fractionation of organic matter aggregates occurs, leading to two pools of organic matter, a dissolved one and an adsorbed one, each one with different structural and chemical properties. Previous studies have shown the influence of this fractionation on the modification of structures and moieties on humic molecules. Generally, these studies analyze the dissolved organic fraction only, which stays in the supernatant after centrifugation of the mixture. The modification of UV/Visible parameters (such as SUVA, E_2/E_3, or ε_{280}) gives information on aromaticity of molecules: all studies show a preferential adsorption of molecules with higher aromaticity (Chorover and Amistadi 2001, Claret et al. 2008, Gu et al. 1995, Meier et al. 1999, Reiller et al. 2006, Zhou et al. 2001). The apparent molecular weight (MW) of non-sorbed fraction has also been studied, using size-exclusion chromatography (SEC). Majority of studies have shown a preferential adsorption of higher MW fractions of various NOM extracts on goethite at pH between 4 and 7.5 (Chorover and Amistadi 2001, Meier et al. 1999, Zhou et al. 2001). However opposite results are reported, for instance Hur and Schlautman (2004) have shown that the apparent MW of non-sorbed fractions of purified Aldrich humic acid onto hematite was pH dependent: below the point of zero charge (i.e. pH=8), high MW fractions are enriched in the solution and apparent lower MW at higher pH. This is consistent with the work of Reiller et al. (2006) which observed a preferential adsorption of low molecular weight (m/z) fraction using ESI-MS with the same system at pH 7. Kang and Xing (2008) proposed a 3 steps scenario for sorption onto goethite : (1) electrostatic attraction or outer-sphere complexation of the polar functional moieties on relatively small and intermediate MW HA fractions (2) ligand exchange of the carboxylic groups of the HA to yield inner-sphere complexes; and (3) hydrophobic interactions on the HA-goethite complex that can provide new

hydrophobic sorption sites for high MWHA fractions with condensed aromatic or long chain aliphatic moieties. The proposition of a generic trend for size modification of HS molecules after adsorption onto oxides minerals is not straightforward. For Al_2O_3 nanoparticles the influence of pH, which seems of great importance, and structural modifications of the HS fractions after adsorption onto a mineral oxide were evidenced (Ghosh et al. 2008; Ghosh et al. 2010). However, to our knowledge, no study has yet looked at the modification of reactivity of the produced organic fractions, which could explain the difficulty to model the behavior of ternary systems composed of pollutants/HS/mineral. The behavior of the pollutant in a ternary system cannot be described by linear additivity of binary systems, due to the interactions between natural organic matter and mineral surfaces, which modify the surface properties, aggregation, and metal ion complexation (Christl and Kretzschmar 2001, Robertson and Leckie 1994, Vermeer et al. 1999). It is actually difficult to access to the binding properties of the dissolved fraction of HS, due to its low concentration in solution after the adsorption experiments. Recent works (Dryer et al. 2008, Janot et al. 2010) have described a new spectrophotometric titration approach, which allows the assessment of the reactivity of HS in solution at relevant environmental concentration (i.e. <10 mg_{HS}/L).

The aim of this study is to use this spectrophotometric titration approach to study dissolved fractions of HS after adsorption experiment, in order to quantify modifications of their binding moieties due to the contact with the mineral surface.

In this work the modifications of reactivity of Purified Aldrich Humic Acid (PAHA) fraction left in solution after adsorption onto α-Al_2O_3 at different organic/mineral ratios are qualitatively characterized. HS adsorption onto oxides has mostly been studied with Fe oxides. α-Al_2O_3 was chosen since aluminol surface sites of Al oxides are part of clay mineral reactive sites. In addition, α-Al_2O3 has significant industrial applications (abrasive agent, insulator, and catalyst) that could lead to environmental exposure. The behavior of man-made nanoparticles exposed to a natural aquatic environment will be controlled by their interactions with natural organic matter which could dictate their bioavailability and toxicity to aquatic species. The quantification of PAHA adsorption onto α-Al_2O_3 depending on pH and initial PAHA concentration was studied by batch experiments. An attempt to access reactivity of the adsorbed PAHA fraction is proposed.

2 Materials and methods

2.1 Preparation of samples

Commercial Aldrich humic acid was purified (PAHA) according to Kim et al. (1990). A stock suspension at 5 g_{PAHA}/L was prepared by diluting PAHA in NaOH (pH around 10) to promote

complete PAHA dissolution. In this work, concentrations of PAHA solutions, noted in mg/L, always correspond to mg_{PAHA}/L.

Alumina (α-Al_2O_3) was purchased from Interchim (pure 99.99%, size fraction 200–500 nm). The solid was washed thrice with carbonate-free NaOH and thrice with freshly produced milli-Q water before drying and storage at room temperature under N_2 atmosphere according to Alliot et al. (2005). Specific area has been found at 15 m^2/g using N_2-BET method, and the pH_{PZC} has been measured at 9.6 (Janot et al., 2011) by potentiometric titration (Hiemstra et al., 1989) (data not shown) as the intersection of titration curves and verified by zeta potential measurements (pH_{IEP} found at 9.5 in 1 g/L α-Al_2O_3, data not shown).

2.2 Adsorption experiments

Suspensions of 1 g/L α-Al_2O_3 with varying PAHA concentration, ionic strength *I* ($NaClO_4$) and pH were made in 10.4 ml Beckman centrifugation tubes (355603). After 3 days of equilibration, final pH was measured and solutions were ultra centrifuged (60 000 rpm for 2 h).

PAHA concentrations in the supernatant were measured using a Shimadzu TOC-VCSH analyzer for data at 0.1 M $NaClO_4$ and for the adsorption isotherm at pH 4, using PAHA as a standard between 0 and 50 mg/L; standard deviation is 0.6 mg/L. For other data sets (at 0.01 M and isotherms at pH 6.2 and 7.4) a carbon contamination was observed in the storage tubes. This contamination was due to inadequate storage of the solutions in plastic tubes that leaked organic carbon measurable with the TOC-VCSH. PAHA concentrations in the supernatants were then determined by UV measurements, with PAHA calibration. UV measurements are known to induce a bias on adsorbed HS quantification, due to the modification of chromophores with fractionation, especially at low humic concentration (Claret et al. 2008, Gu et al. 1996). A non-contaminated set of supernatant solution has then been used as reference to choose the wavelengths of calibration in order to minimize the difference between UV and DOC measurements. For each wavelength between 220 and 600 nm, calibration curves were determined. Best results were found when using the mean of values obtained from wavelengths between 290 and 320 nm (see Figure S1 of the supplementary information (SI)).

2.3 LC-OCD measurements

The LC-OCD system (DOC-LABOR Dr. Huber, Germany) is equipped with a size exclusion column TSK HW50S (Tosoh, Japan) and an online organic carbon detector. After the injection of a water sample, organic compounds in the sample are separated by the size exclusion unit according to their molecular size. Thereafter, the separated organics are oxidized sequentially and their carbon content is quantified by the online detector. On average, the ratio of the chromatogram DOC, i.e., total

DOC analyzed after SEC chromatography, to the DOC analyzed using a TOC analyzer (Shimadzu TOC-VCSH) is over 85%. Thus, the component analysis based on LC-OCD chromatograms is considered to be able to represent the fraction distribution in the water samples. For data acquisition and data processing, the customized software ChromCALC® is used. According to the study of Huber et al. (2011) and with the assistant of the software, 4 major components from the chromatograms are identified in the present work: colloidal + macromolecular humics, building blocks, low molecular weight acids and neutrals. Before measurement, the system was calibrated according to the methods described by Huber et al. (2011). According to Shimadzu results, the water samples are diluted using mQ water to a DOC of 1 to 3 mg/L prior to LC-OCD measurement. Accordingly, PAHA stock solution was diluted 100 times and the supernatants from adsorption experiments were diluted with a factor of 3. Calibration of organic carbon measurements being different from the one used for adsorption quantification, results can then not be compared directly.

2.4 Titration experiments

A series of retention experiments at 10 g/L α-Al_2O_3 and various initial PAHA concentrations (600, 300, 200, 120 and 70 mg/L), I = 0.1 mol/L ($NaClO_4$), pH = 6.8 ± 0.3, and 5 days of equilibration was also done. For each PAHA concentration, at least three replicates were made. The supernatants were mixed and the solution was diluted in 0.1 mol/L ($NaClO_4$) to obtain a 100-mL solution of 10 mg/L, which was then titrated between pH 3 and pH 11 using the spectrophotometric method described in Janot et al. (2010). Spectrophotometric titrations allow access to the reactivity of a dilute solution of humic substances (HS) due to the variations in UV/Vis spectra of the solution with evolving pH. The pH was increased by addition of freshly prepared NaOH at 0.01 or 0.1 mol/L. Absorbance spectra were recorded in a 5 cm quartz cuvette at ca. 0.5 pH intervals using a Thermo Evolution 600 UV/Visible spectrophotometer between 190 and 600 nm. UV/Visible spectra were recorded at room temperature. PAHA concentrations in the supernatant were measured using Shimadzu TOC-VCSH analyzer.

3 Results and Discussion

3.1 Influence of solution parameters on PAHA adsorption

Quantification of PAHA adsorption onto α-Al_2O_3 was made at different pH, for a coverage ratio R = 25 $mg_{PAHA}/g\alpha\text{-}Al_2O_3$. Humic acid adsorption onto oxides reported in the literature show a surface concentration up to 4.5 mg_{HA}/m^2, depending on mineral, ionic strength, pH and initial coverage ratio (Boily and Fein 2000, Fairhurst and Warwick 1998, Hur and Schlautman 2004, Murphy et al. 1999, Reiller et al. 2002, Schlautman and Morgan 1994, Weng et al. 2007). Our results showed a typical

decrease of PAHA retention onto α-Al_2O_3 with increasing pH (see Figure 1), from 1.24 mg/m² at pH 4.0 (i.e., 76% of initial amount of PAHA) to 0.61 mg/m² at pH 8.8 (i.e., 37%).

As previously observed for simple organic acids, the sorption of acid anions is linked to their protonation constant (Evanko and Dzombak 1998). From potentiometric titrations data of PAHA, the median intrinsic affinity parameters were found at $\log\tilde{K}_{H,1} = 2.66$ and $\log\tilde{K}_{H,2} = 6.90$ (Janot et al. 2010), which gives maximum of affinity distribution around 5.0 and 9.2 at 0.01 M and 4.5 and 9.7 at 0.1 M, respectively. The distribution of affinity constants ($\tilde{K}_{H,i}$) due to the PAHA heterogeneity induces a monotonous decrease of the sorption. At low pH (< 5), inner-sphere complexation occurs between deprotonated carboxylic ligands of PAHA and positively charged surface groups of the oxide (Weng et al, 2007). When pH increases, the net positive charge of alumina surface is decreasing and the more negatively charged PAHA is less attracted to it. The high point of zero charge of the surface, i.e. 9.6, also explains the significant amount of PAHA bound throughout the pH range studied.

Despite the low number of data at 0.01 M, adsorption of PAHA also seems to be slightly depend on ionic strength (see Figure 1), with amount of PAHA adsorbed decreasing with ionic strength above pH 5. Weng et al.(2007) made the same observations for a HA/goethite system, in the same surface coverage conditions: 150 mg_{HA}/L with 1 g/L of goethite with a 94 m²/g specific area, i.e. 1.60 mg_{HA}/m^2 when we used 1.66 mg_{HA}/m^2 in our experiment. Weng et al.(2007) also noticed no difference in HA surface concentration between 0.1 M and

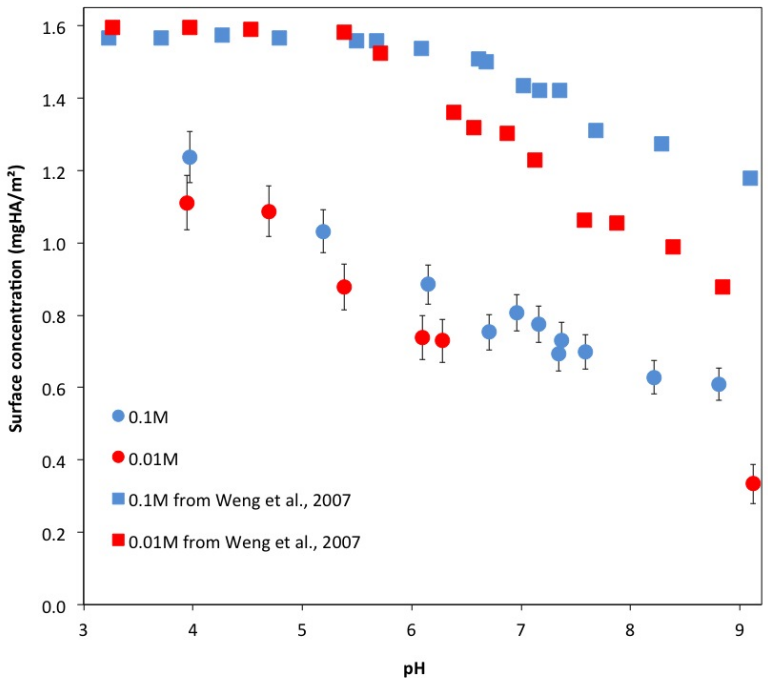

Figure 1. *Influence of pH and ionic strength on PAHA adsorption onto α-Al_2O_3. Re-calculated data from Weng et al. (2007) for HA adsorption onto goethite have been plotted for comparison.*

dx.doi.org/10.1016/j.watres.2011.11.042

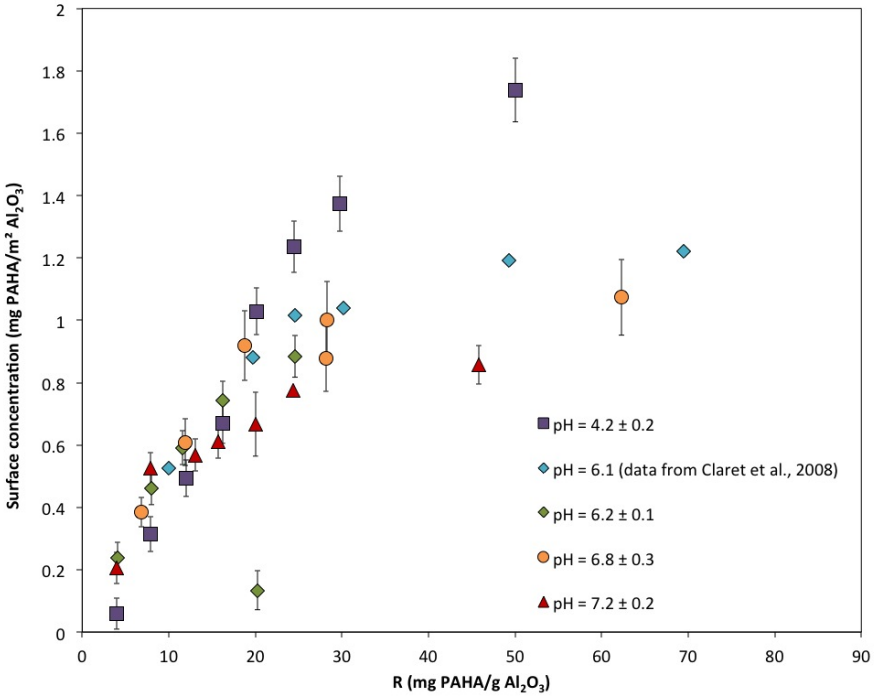

Figure 2. *PAHA surface concentration depending on pH and initial concentration. Error bars correspond to σ.*

0.01 M $NaNO_3$ below pH 5.7, but a lower adsorption of HA at 0.01 M $NaNO_3$ for higher pH values. Their results are plotted on Figure 1 for comparison. Sakuragi et al. (2004) reported the same behavior for humic acid adsorption onto hematite between 0.05 and 0.5 M. When ionic strength increases, the Donnan volume of the humic molecules and the electrostatic repulsion between charges decrease, allowing molecules to move closer to the surface and leading to an increase of adsorbed PAHA amount. Conversely, Filius et al. (2000) and Reiller et al. (2002) did not report salt effects for fulvic acid adsorption on goethite. The influence of electrostatic effects is explained by both the tendency to form aggregates and the larger size of humic acid molecules, their conformation being more dependent on ionic strength than the fulvic acids one (Saito et al. 2004).

The influence of PAHA initial amount (10 g/L of α-Al_2O_3, 5 days of equilibration) was studied at pH 6.8 ± 0.3. Results are shown in Figure 2, together with the results from Claret et al. (2008) obtained for the same system (same concentration of α-Al_2O_3, pH = 6.1 ± 0.1 and 24 h of contact). The two data sets are consistent, which shows that equilibration time has almost no influence on PAHA adsorption between 1 and 5 days, at least regarding the total carbon adsorbed. This isotherm is also compared with three other experiments performed at 1 g/L α-Al_2O_3 and pH = 4.2 ± 0.2, 6.2 ± 0.1, 7.2 ± 0.2 (see Figure 2). The three points at R = 25 $mg_{PAHA}/g\alpha\text{-}Al_2O_3$ are taken from the pH-isotherm shown in Figure 1.

Except for the point corresponding to pH 6.2 and 20 $mg_{PAHA}/g\alpha\text{-}Al_2O_3$, which can be considered erroneous, PAHA adsorption onto α-Al_2O_3 at different pH follows the same trend.

The adsorption isotherms show an increase with increasing initial quantity, until a plateau is reached. This saturation threshold decreases with increasing pH, which is commonly found in the case of HS adsorption onto metal (hydr)oxides (Filius et al. 2000, Kang and Xing 2008, Saito et al. 2004, Schlautman and Morgan 1994, Vermeer et al. 1998). Saturation is reached for a lower R value at higher pH.

3.2 Characterization of supernatants

UV/Visible measurements were made on the supernatants from adsorption isotherm at pH 6.8 and 10 g/L α-Al_2O_3. UV/Visible spectra of NOM samples can provide some structural information. $SUVA_{254}$ (Specific UV Absorbance at 254 nm) values are summarized in Table 1, together with the ratio of absorbance values at 254 and 365 nm (E_2/E_3) and the half-width of the electron-transfer band (Δ_{ET}, in electron-volt) as described by Korshin et al. (1999). These values have been measured for the original PAHA solution as well as for the different supernatants.

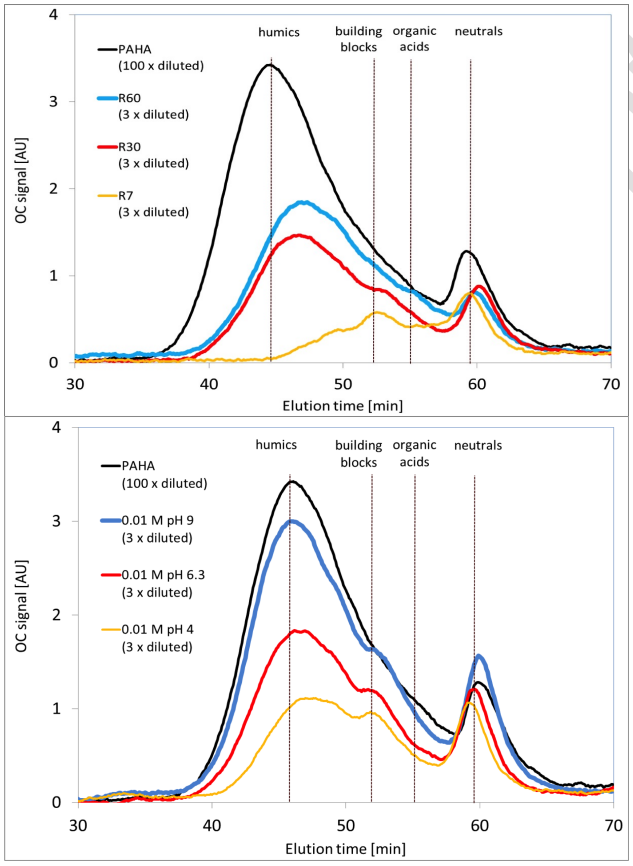

Figure 3. *LC-OCD chromatograms of PAHA and of supernatants from adsorption experiments (A, top) at 0.1M and pH ≈ 6.8 (R in $mg_{PAHA}/g\alpha\text{-}Al_2O_3$) and (B, bottom) at 0.01M and different pH (R ≈ 25 $mg_{PAHA}/g\alpha\text{-}Al_2O_3$).*

Table 1. *Parameters of UV absorbance spectra of the different samples (at pH = 6).*

	$SUVA_{254}$ (mg^{-1} L m^{-1})	Δ_{ET} (eV)	E_2/E_3
PAHA	5.0	2.5	3.0
R = 60 mg/g	5.5	2.4	3.3
R = 30 mg/g	6.2	2.5	3.1
R = 20 mg/g	5.4	2.4	3.3
R = 12 mg/g	3.9	2.0	5.8
R = 7 mg/g	2.3	1.9	6.5

The three parameters shown in Table 1 are almost constant for $20 \leq R \leq 60$ mg_{PAHA}/g and comparable to the values of original PAHA at the same pH and ionic strength. For $R < 20$ $mg_{PAHA}/g\alpha\text{-}Al_2O_3$, i.e. highest fractionation rates, $SUVA_{254}$ is decreasing. Previous studies have shown that aromaticity is correlated to $SUVA_{254}$ as well as Δ_{ET} (Chin et al. 1994, Korshin et al. 1999, Weishaar et al. 2003) and anti-correlated to E_2/E_3 (Peuravuori and Pihlaja 1997). In our case, it means that PAHA fractions in solution for concentration ratios below 20 $mg_{PAHA}/g\alpha\text{-}Al_2O_3$ show a loss of

dx.doi.org/10.1016/j.watres.2011.11.042

Table 2. *Percentage content of different fractions in water sample before and after adsorption as measured by LC-OCD. Definition for humics, building blocks, organic acids and neutrals can be found in Huber et al, (2011).*

PAHA solution	humics	building blocks	organic acids	neutrals
	[%]	[%]	[%]	[%]
Raw solution	73.7	14.3	3.8	8.2
R60 0.1 M pH 6.8	69.6	8.9	3.6	17.9
R30 0.1 M pH 6.8	62	12	6	22
R7 0.1 M pH 6.8	26.9	23.1	11.5	38.5
R25 0.01 M pH 9	64.2	8.4	5.3	22.1
R25 0.01 M pH 6.3	58.6	7.1	5.7	28.6
R25 0.01M pH 4	54.9	5.9	5.9	33.3

aromaticity regarding to original PAHA. The same observation was made by Claret et al. (2008) for the same system after adsorption at pH = 6.1, with a decrease observed for $R < 10\ mg_{PAHA}/g\alpha\text{-}Al_2O_3$ (see Figure S2). The preferential adsorption of more aromatic HA fraction is in agreement with literature data (Chorover and Amistadi 2001, Claret et al. 2008, Gu et al. 1995, Meier et al. 1999, Reiller et al. 2006, Zhou et al. 2001).

LC-OCD measurements were performed on the same samples. Figure 3A shows the chromatograms obtained, with the organic carbon signal depending on elution time, larger aggregates being eluted faster. Table 2 shows the DOC contribution of the different components of each sample. The content of humic substances in the supernatants is significantly reduced by decreasing the coverage ratio R. The behavior of specific DOC fractions is different in adsorption process. With respect to the humics (elution time to 50 min, see Figure 3A), the decrease of PAHA initial load results in a decrease of the relative content of this fraction, from around 70% to 27% (see Table 2). This indicates the preferential removal of humics after adsorption onto $\alpha\text{-}Al_2O_3$. A preferential adsorption of larger molecules is occurring: when coverage ratio decreases, the peak observed around 43 min is delayed, indicating a loss of larger molecules in solution after centrifugation of the samples. This peak is decreasing with R value. This observation is in agreement with spectroscopic measurements and decrease of Δ_{ET} value with R: Korshin et al. (1999) noted a correlation between Δ_{ET} value and gyration radii of humic molecules obtained by low-angle X-ray diffraction. Different to the behavior of the humics fraction, decreasing R results in an increase of the relative content of all the other smaller organics, e.g. building blocks, organic acids and neutral substances

(see Figure 3A and Table 2). This phenomenon implies that, compared to humics, these small organics are not as readily adsorbed onto the minerals under the present experimental conditions. Specially, as neutral organics are of very low UV absorbance (Huber et al. 2011), the increase of their relative content should reduce the SUVA of water samples, which is in agreement with observations (see Table 1 and Figure S2).

LC-OCD measurements were also performed on the supernatants of adsorption experiments at 0.01 M $NaClO_4$ and different pH values (macroscopic results shown in Figure 1). Results are shown in Figure 3B and Table 2. The analysis of fractionated DOC shows that when pH decreases and more PAHA is adsorbed onto the surface (Figure 1), the relative content of humics and building blocks (which are considered as break down products of humics) is decreasing (see Table 2): these fractions are preferentially adsorbed onto the mineral. Although the organic acids can also be removed, their relative content remains constant. Again, an ineffective removal of the neutrals increases their relative content in the residual DOC.

The LC-OCD analysis of these two series of supernatants shows that humics and humic-like substances (building blocks) have a similar behavior and are preferentially adsorbed onto the mineral surfaces in various conditions of pH, ionic strength and coverage ratio. For instance the building blocks could actually corresponds to the highly polar short-chain carboxylic acids identified by Ghosh et al. (2010) that could react with the surface mostly by ligand exchange of the carboxylic groups of the HA to yield inner-sphere complexes (Kang and Xing, 2008) and lateral interactions (Ochs et al., 1994).

Kinetic aspects of the process could also be important. For instance Van de Weerd et al. (1999) interpreted the data of Gu et al. (1994) from a kinetic point of view. The smaller molecules move faster and could thus be favored and slowly exchanged for the bigger ones. However, the ranges of molecular weights (from <3 kDa to >100 kDa) used in both papers rely on the determination by McCarthy et al. (1993) based on ultrafiltration membranes calibrated with globular proteins. These calibrations give high molecular weight values because of the compact structure of proteins (Chin and Gschwend, 1991; Chin et al., 1994). As we did not perform the same molecular mass determinations, the direct comparison would then be tricky.

3.3 Spectrophotometric titrations

The differential absorbance spectra of all the supernatants were calculated as described by Janot et al. (2010). Briefly, they are built from the absorbance spectra of PAHA solution recorded at different pH between 3 and 11, using the following equation:

$$\Delta A_{pH}(\lambda) = \frac{1}{l_{cell}}\left[\frac{A_{pH}(\lambda)}{DOC} - \frac{A_{pH_{ref}}(\lambda)}{DOC_{ref}}\right]$$

where l_{cell} is the cell length (cm), DOC and DOC_{ref} (mg/L) are the dilution-corrected concentrations of DOC in the solution at the pH

dx.doi.org/10.1016/j.watres.2011.11.042

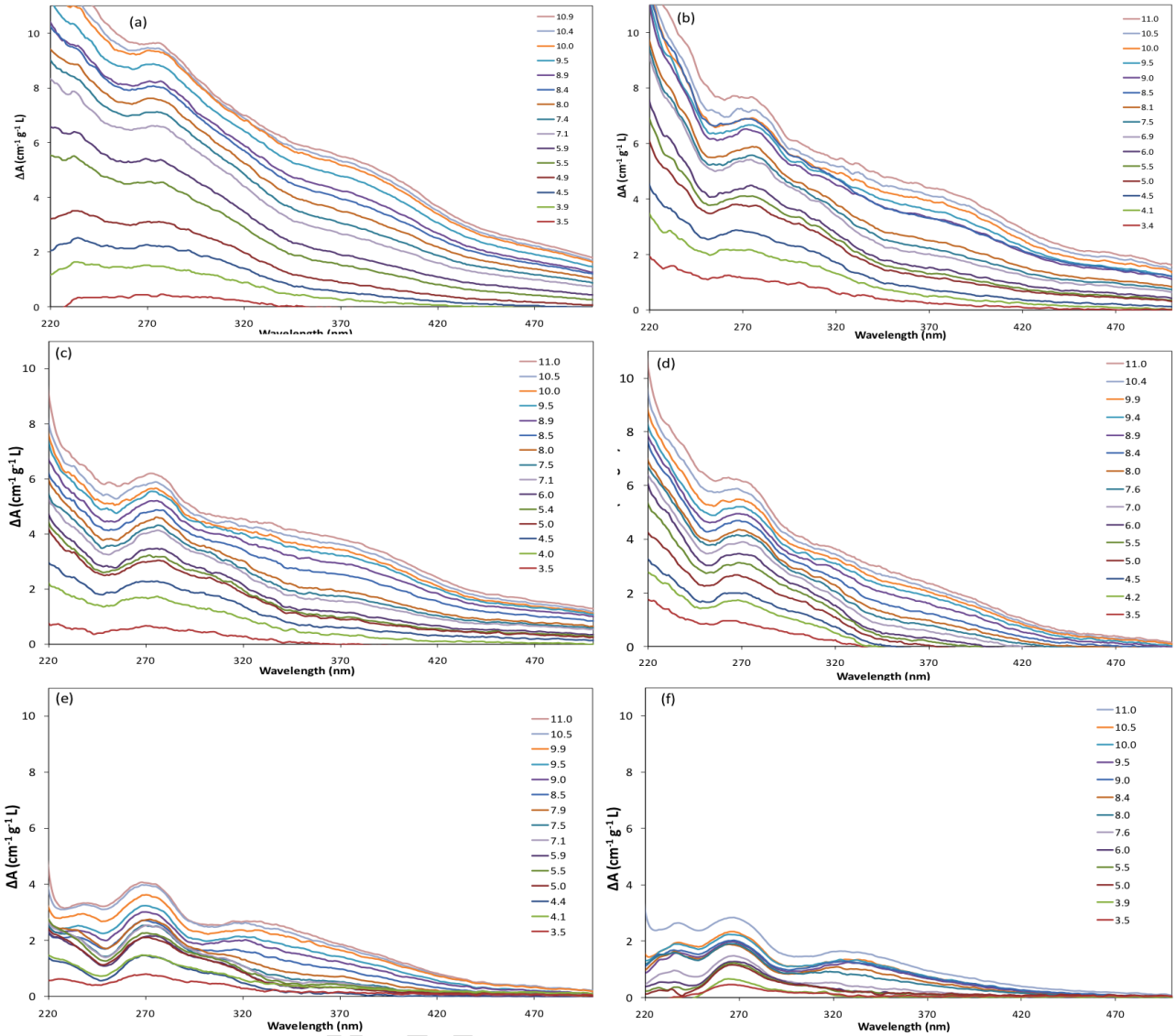

Figure 4. *Differential absorbance spectra of supernatants from retention experiments ($pH_{ref} \approx 3.0$) for (a) original PAHA and different organic/mineral ratios (b) R = 60 mg/g (c) R = 30 mg/g (d) R = 20 mg/g (e) R = 12 mg/g (f) R = 7 mg/g.*

of interest and at the chosen reference pH, respectively. $A_{pH}(\lambda)$ and $A_{pHref}(\lambda)$ are the absorbance values measured at a given wavelength λ at the pH of interest and at the reference pH, respectively.

The spectrum recorded at the lowest pH value, i.e., $pH_{ref} \backsimeq 3$, is used as a reference to examine the evolution of differential spectra throughout the entire pH range. The results of differential absorbance spectra of the supernatants for different initial coverage rates are shown in Figure 4. The main evolution is the decrease of differential absorbance values with decreasing R value, at all the wavelength studied. The lack of differences in solution properties at high HS/surface ratio is accounted for by the small percentage of PAHA removed from the solution to the mineral surface (16%). In this situation big changes are not expected to be observed even if there is preferential adsorption of certain molecules. The effects are expected to become

dx.doi.org/10.1016/j.watres.2011.11.042

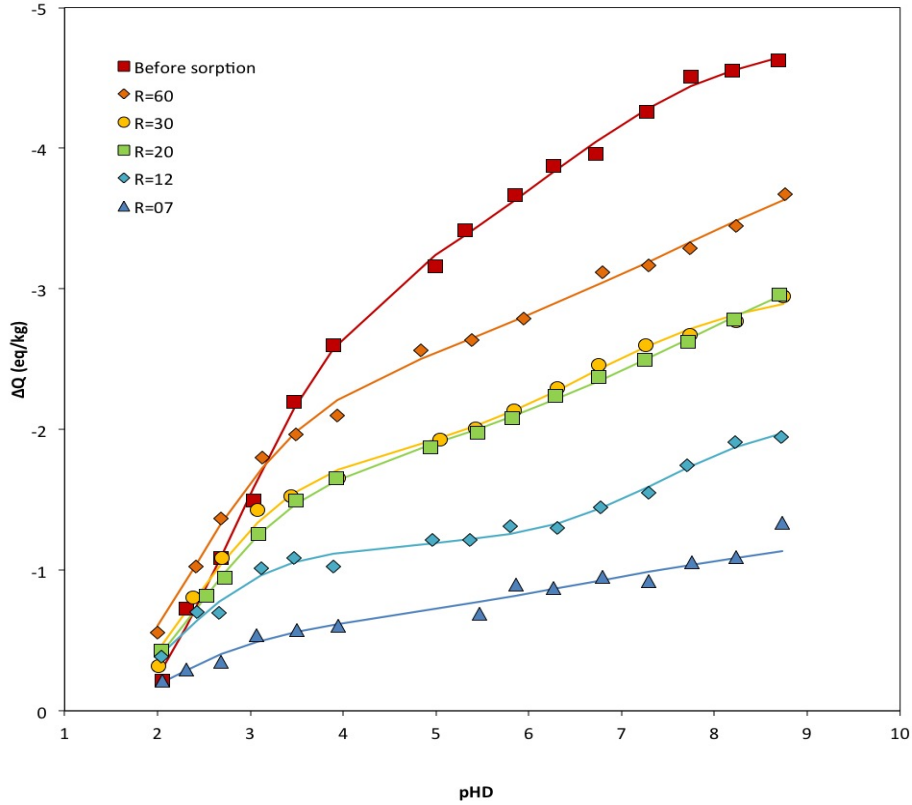

Figure 5. *Calculated charge curves for the different supernatant titrations (symbols), depending on pH in the Donnan gel, and the corresponding fits (lines).*

bigger at lower loading as observed in Figure 4. Deprotonation induces less change in the UV/Visible spectra for PAHA fractions compared to the original PAHA. This can be related to the loss of proton binding sites. The modification of the different features on the differential absorbance spectra are clearly visible too, especially the loss of the broad range around 370 nm, leading to the apparition of a 330 nm-centered feature for the two lowest R values.

Titration curves were built using the values of differential absorbance at 270 nm vs pH. This value is increasing with pH and decreasing with R. The transformation from spectrophotometric data to titration curves may be found elsewhere (Janot et al. 2010). The electrostatic correction previously determined has been applied to these titration curves, and the corresponding charges was calculated using the transfer function obtained for un-fractioned PAHA (Janot et al. 2010). This function can be used here as we are in the same conditions of ionic strength and using the same HA. It should be mentioned however that fractionation may induce modifications to this operational transfer function, which are not characterized. Results of charge calculations in function of pH and coverage ratio are shown in Figure 5. The charging per unit carbon decreases with decreasing loading and lowering of pH. This is in agreement with the thermodynamic model as put forward by Weng et al. (2007).

3.4 Modeling

Data modeling was done within the NICA-Donnan formalism (Kinniburgh et al. 1999), optimizing the parameters with the software FIT (Kinniburgh 1993). The number of data points in the spectrophotometric titration curves is much lower than in the potentiometric ones (80 vs 15). The parameters describing the charge vs. pH_{Donnan} curve for the original sample (before adsorption) were re-calculated using spectrophotometric data, for the sake of comparison with data from adsorption experiments. First, to constrain the calculation, Q_0 for the original sample, i.e., the initial residual charge of the PAHA or reactive sites not titrated, was set equal to the value found in potentiometric modeling, i.e., 0.6 eq/kg. This corresponds to 13% of ΔQ_{max}, where Q_{max} is the maximum number of titrated reactive sites. It is assumed that the proportion of Q_0 / ΔQ_{max} was specific of PAHA, and for all the samples Q_0 values were fixed at 13% of the corresponding ΔQ_{max}.

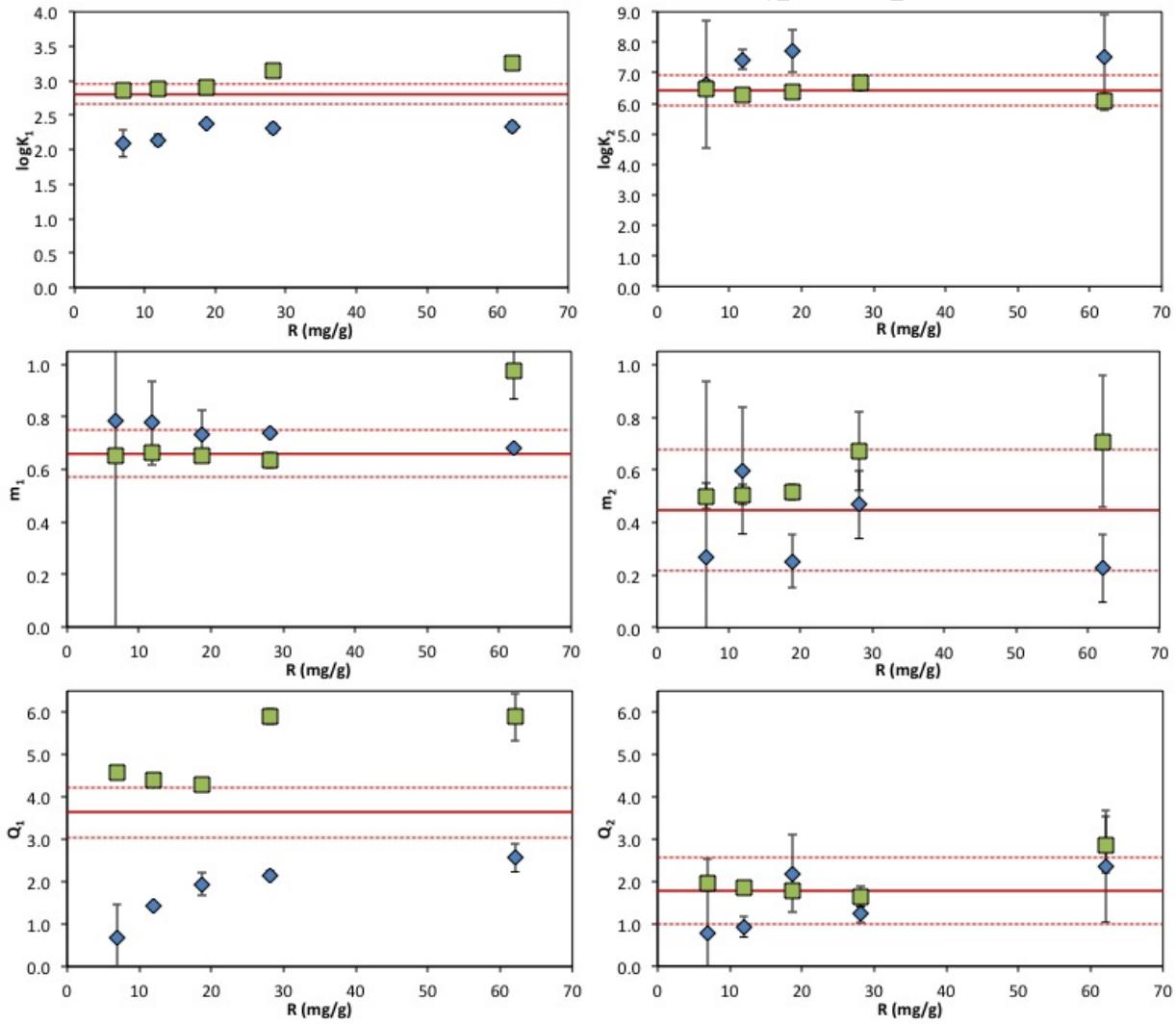

Figure 6. *NICA-Donnan parameters for the dissolved (blue) and adsorbed (green) fractions of PAHA, compared to the initial value (red line). Errors bars are equal to σ.*

The obtained fitting are satisfactory for all samples ($r^2 > 0.98$), but for 60 and 30 $mg_{PAHA}/g\alpha\text{-}Al_2O_3$ the best fit was obtained for m_1 values larger than 1, which is difficult to explain within the framework of the model and known titrations data of various humic substances from the literature (Milne et al. 2001). Values of m_1 below 1 for these two ratios were optimized between neighboring values, since m_1 seems to increase when R decreases. The obtained parameters are shown in Table S1 of SI and the corresponding fits are displayed on Figure 5.

The overall charge $Q_1 + Q_2$ decreases with the initial quantity of PAHA in the system, most of the reactive molecules being retained onto the mineral surface, their functional sites being directly fixed to the surface mostly via ligand exchange (Ochs et al. 1994; Kang and Xing, 2008).

For the sake of clarity, the evolution of NICA-Donnan parameters with R and comparison to initial PAHA are plotted in Figure 6 (blue symbols). The progressive decrease of Q_1 with R shows a preferential adsorption of the molecules bearing the most reactive moieties. At experimental pH, i.e., 6.8 ± 0.3, around 96 % of low proton-affinity-type (so-called carboxylic) sites are deprotonated and more easily retained onto the positively-charged alumina surface, which results in a non-sorbed PAHA fraction depleted in these moieties. It is also in agreement with the preferential sorption of highly polar short-chain carboxylic acids during humic acid sorption onto colloidal Al_2O_3 evidenced by Ghosh et al. (2008, 2010). There is no apparent evolution of the number of high proton-affinity-type (so-called phenolic) sites Q_2, which seems to be constant above $R = 20\ mg_{PAHA}/g\alpha\text{-}Al_2O_3$ and not significantly different from the original PAHA. However, it is lower for remaining PAHA fraction in solution at the two lowest ratios. This is consistent with the loss of aromaticity observed from the UV/Visible spectra for these supernatants (see Figure S2). The heterogeneity parameter m_1 increases with decreasing ratio. This would mean that low proton-affinity-type sites of PAHA fraction in solution are more homogeneous than initial PAHA. When fractionation is more important, the apparent homogeneity of low affinity-type sites increases too.

The $\log\tilde{K}_{H,1}$ values of supernatant fractions seem to slightly decrease with coverage ratio, which would mean a higher affinity for proton and a greater tendency for deprotonation. Previous works related to the adsorption of simple organic acids onto mineral oxides have shown that adsorption is maximal at the pH corresponding to the pK_a of the acid (Gu et al. 1995, Schulthess and McCarthy 1990). Some of these molecules, often considered as analogs of humic substances, show a maximum of adsorption below pH 4: it is the case of benzoic acid onto goethite (Evanko and Dzombak 1998), phtalic acid onto hematite (Gu et al. 1995) or salicylic acid onto δ-alumina (Kraemer et al.

dx.doi.org/10.1016/j.watres.2011.11.042

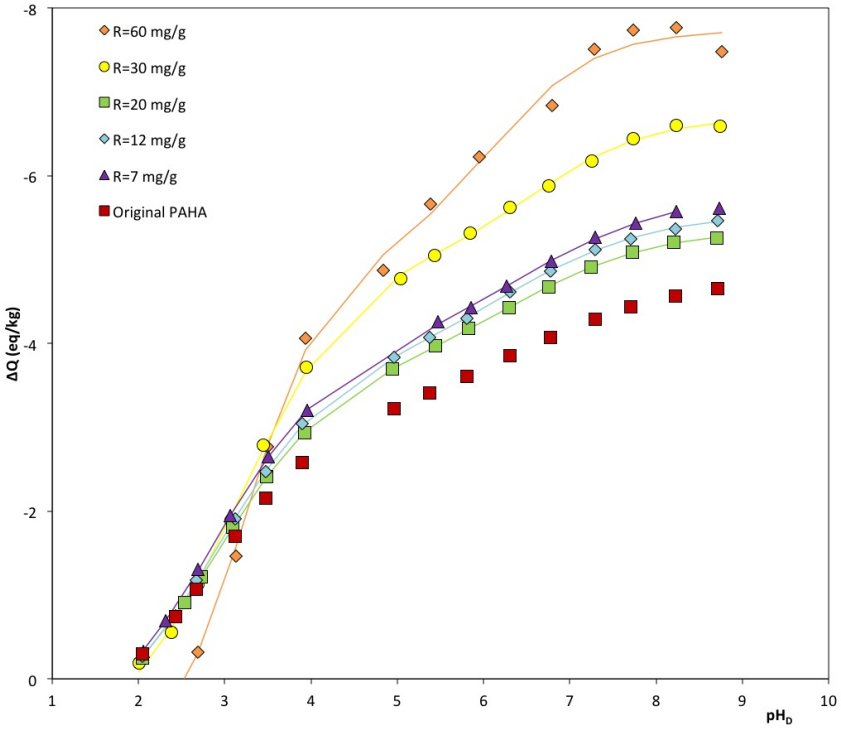

Figure 7. *Calculated charge curves for adsorbed fractions of PAHA.*

1998). For these molecules, there is almost no more adsorption at pH higher than 6. By analogy, at the pH of our experiment (6.8), these molecules would be very weakly sorbed. The lower value of $\log\tilde{K}_{H,1}$ for the humic molecules found in the supernatants regarding the original value may be related to the presence in these humic molecules of such organic moieties with very low pK_a (3.0 for salicylic acid, 4.2 for benzoic acid and 2.9 for the first pK_a of phtalic acid).

We can not conclude regarding the evolution of m_2, since its values are too close from the original value. This is due to experimental pH 6.8 under which the majority of phenolic-type sites are not deprotonated ($\log\tilde{K}_{H,2}$ = 8.7 at I = 0.1 M). Thus only experiments made at very low R values would allow the more definitive conclusions on m_2 evolutions. Regarding the evolution of $\log\tilde{K}_{H,2}$ it is again difficult to conclude since values seem higher in the non-sorbed PAHA molecules than in the original bulk PAHA.

In addition, it must be highlighted that these parameters are fitted from 15-points data sets, and that the correlation matrices show a strong correlation between Q_1, m_2 and Q_2, as shown in Table S2.

In order to study the modifications of PAHA reactivity in the two fractions due to adsorption, the charging behavior of adsorbed PAHA fraction is still missing. From DOC measurements, the proportion of dissolved and adsorbed fractions can be calculated for each coverage ratio. It is then possible, from mass balance data, to calculate the charge of the adsorbed PAHA fraction. Results are plotted in Figure 7.

dx.doi.org/10.1016/j.watres.2011.11.042

Site densities of adsorbed fractions are higher than the ones of the original PAHA: most reactive fractions are preferentially adsorbed onto the oxide surface. Before saturation of the surface is reached, i.e. $R < 30\ mg_{PAHA}/g\alpha\text{-}Al_2O_3$ (see Figure 2), there is almost no difference between charging behavior of adsorbed fractions. But once saturation is reached, charge is increasing with R.

The modeling of the charging curves, to characterize an evolution of the NICA-Donnan parameters of these fractions is then done as previously for the fraction in solution (Figure 6). The evolutions of the different parameters with initial coverage ratio R, compared to the results for dissolved fraction and original material, are shown in Figure 6 (green symbols). The $\log\tilde{K}_{H,1}$ values of PAHA adsorbed fractions are similar to the ones of original PAHA for $R < 30\ mg_{PAHA}/g\alpha\text{-}Al_2O_3$. For the highest R values, when saturation of the surface is reached, the $\log\tilde{K}_{H,1}$ values slightly increase, while the apparent homogeneity of the low-affinity sites distribution m_1 increases too. The charge is always higher in the adsorbed fraction than in the original material. The quantity of low affinity-type sites is always significantly higher in the sorbed fraction than in the dissolved one, due to the preferential adsorption of fractions bearing the most reactive moieties, i.e., short-chain carboxylic acids. The saturation is reached for $Q_1 = 6$ eq/kg.

There is no apparent evolution of both the $\log\tilde{K}_{H,2}$ and m_2 values that are comparable to the value of original PAHA. They are inside the statistical envelope $m_2 \pm \sigma(m_2)$ of the original PAHA. This would mean that the functional sites in the adsorbed fraction are more homogeneous when saturation is reached.

From these measurements it appears that, under our conditions at pH ≈ 6.8, fractionation due to adsorption of PAHA onto $\alpha\text{-}Al_2O_3$ mostly impact the low proton-affinity type sites, which are almost totally ionized. The lack of trend for high proton-affinity-type sites behavior may be due to the slight variations of pH value between the different batch solutions, which have a large impact on the ionization of these functional sites at the chosen experimental pH.

4 Conclusions

Differential spectrophotometric measurements have been proved useful to study variations of PAHA protonation behavior due to adsorption onto a mineral surface. However, it seems essential to have titration curves with more data points, in order to have better constrained fits. It would also be important to do the same study at different experimental pH, in order to characterize PAHA reactivity modifications due to adsorption throughout a large pH range. The LC-OCD analysis shows that humics and humic-like substances (building blocks) are preferentially adsorbed onto the mineral surfaces in various conditions of pH, ionic strength and coverage ratio. The amount of low-proton-affinity type of sites and the value of their median affinity constant decrease after

adsorption. These changes in reactivity to our opinion could explain the difficulty to model the behavior of ternary systems composed of pollutants/HS/mineral since additivity is not respected. Model of ternary systems should explicitly take into account the different reactivity of both fractions.

Supplementary material

Supplementary material associated with this article can be found, in the online version, at doi:10.1016/j.watres.2011.11.042.

REFERENCES

Alliot, C., Bion, L., Mercier, F. and Toulhoat, P. (2005) Sorption of aqueous carbonic, acetic, and oxalic acids onto alpha-alumina. Journal of Colloid and Interface Science 287(2), 444-451.

Boily, J.F. and Fein, J.B. (2000) Proton binding to humic acids and sorption of Pb(II) and humic acid to the corundum surface. Chemical Geology 168(3-4), 239-253.

Chin, Y.P., Gschwend, P.M., 1991. The abundance, distribution, and configuration of porewater organic colloids in recent sediments. Geochimica et Cosmochimica Acta 55 (5), 1309-1317.

Chin, Y.P., Aiken, G. and Oloughlin, E. (1994) Molecular weight, polydispersity, and spectroscopic properties of aquatic humic substances. Environmental Science & Technology 28(11), 1853-1858.

Chorover, J. and Amistadi, M.K. (2001) Reaction of forest floor organic matter at goethite, birnessite and smectite surfaces. Geochimica Et Cosmochimica Acta 65(1), 95-109.

Christl, I. and Kretzschmar, R. (2001) Interaction of copper and fulvic acid at the hematite-water interface. Geochimica Et Cosmochimica Acta 65(20), 3435-3442.

Claret, F., Schafer, T., Brevet, J. and Reiller, P.E. (2008) Fractionation of Suwannee River Fulvic Acid and Aldrich Humic Acid on alpha-Al2O3: Spectroscopic Evidence. Environmental Science & Technology 42(23), 8809-8815.

Davis, J.A. and Gloor, R. (1981) Adsorption of dissolved organics in lake water by aluminum-oxide - effect of molecular weight. Environmental Science & Technology 15(10), 1223-1229.

Dryer, D.J., Korshin, G.V. and Fabbricino, M. (2008) In situ examination of the protonation behavior of fulvic acids using differential absorbance spectroscopy. Environmental Science & Technology 42(17), 6644-6649.

Evanko, C.R. and Dzombak, D.A. (1998) Influence of structural features on sorption of NOM-analogue organic acids to goethite. Environmental Science & Technology 32(19), 2846-2855.

Fairhurst, A.J. and Warwick, P. (1998) The influence of humic acid on europium-mineral interactions. Colloids and Surfaces a-Physicochemical and Engineering Aspects 145(1-3), 229-234.

Filius, J.D., Lumsdon, D.G., Meeussen, J.C.L., Hiemstra, T. and Van Riemsdijk, W.H. (2000) Adsorption of fulvic acid on goethite. Geochimica et Cosmochimica Acta 64(1), 51-60.

Ghosh, S., Mashayekhi, H., Pan, B.; Bhowmik, P., Xing, B. (2008) Colloidal Behavior of Aluminum Oxide Nanoparticles As Affected by pH and Natural Organic Matter. Langmuir, 23, 7024–7031.

Ghosh, S., Mashayekhi, H., Bhowmik, P. and Xing, B (2010) Colloidal Stability of Al_2O_3 Nanoparticles as Affected by Coating of Structurally Different Humic. Langmuir, 26 (2), 873–879

Gu, B.H., Mehlhorn, T.L., Liang, L.Y. and McCarthy, J.F. (1996) Competitive adsorption, displacement, and transport of organic matter on iron oxide .1. Competitive adsorption. Geochimica Et Cosmochimica Acta 60 (11), 1943-1950.

Gu, B.H., Schmitt, J., Chen, Z., Liang, L.Y. and McCarthy, J.F. (1995) Adsorption and desorption of different organic-matter fractions on iron-oxide. Geochimica Et Cosmochimica Acta 59(2), 219-229.

Gu, B.H., Schmitt, J., Chen, Z., Liang, L.Y., McCarthy, J.F., 1994. Adsorption and desorption of natural organic-matter on iron-oxide - mechanisms and models. Environmental Science &Technology 28 (1), 38-46.

Huber, S.A., Balz, A., Abert, M. and Pronk, W. (2011) Characterisation of aquatic humic and non-humic matter with size-exclusion chromatography - organic carbon detection - organic nitrogen detection (LC-OCD-OND). Water Research 45 (2), 879-885.

Hur, J. and Schlautman, M.A. (2003) Molecular weight fractionation of humic substances by

adsorption onto minerals. Journal of Colloid and Interface Science 264(2), 313-321.

Hur, J. and Schlautman, M.A. (2004) Effects of pH and phosphate on the adsorptive fractionation of purified Aldrich humic acid on kaolinite and hematite. Journal of Colloid and Interface Science 277(2), 264-270.

Janot, N., Reiller, P.E., Korshin, G.V. and Benedetti, M.F. (2010) Using Spectrophotometric Titrations To Characterize Humic Acid Reactivity at Environmental Concentrations. Environmental Science & Technology 44(17), 6782-6788.

Kang, S.H. and Xing, B.S. (2008) Humic acid fractionation upon sequential adsorption onto goethite. Langmuir 24(6), 2525-2531.

Kim, J.I., Buckau, G., Li, G.H., Duschner, H. and Psarros, N. (1990) Characterization of humic and fulvic-acids from Gorleben groundwater. Fresenius Journal of Analytical Chemistry 338(3), 245-252.

Kinniburgh, D.G. (1993) FIT Non-linear Optimization Algorithm and User Manual, British Geological Survey, Nottingham, UK.

Kinniburgh, D.G., van Riemsdijk, W.H., Koopal, L.K., Borkovec, M., Benedetti, M.F. and Avena, M.J. (1999) Ion binding to natural organic matter: competition, heterogeneity, stoichiometry and thermodynamic consistency. Colloids and Surfaces a-Physicochemical and Engineering Aspects 151(1-2), 147-166.

Korshin, G.V., Kumke, M.U., Li, C.W. and Frimmel, F.H. (1999) Influence of chlorination on chromophores and fluorophores in humic substances. Environmental Science & Technology 33(8), 1207-1212.

Kraemer, S.M., Chiu, V.Q. and Hering, J.G. (1998) Influence of pH and competitive adsorption on the kinetics of ligand-promoted dissolution of aluminum oxide. Environmental Science & Technology 32(19), 2876-2882.

McCarthy, J.F., Williams, T.M., Liang, L.Y., Jardine, P.M., Jolley, L.W., Taylor, D.L., Palumbo, A.V., Cooper, L.W., 1993. Mobility of natural organic matter in a sandy aquifer. Environmental Science & Technology 27 (4), 667-676.

Meier, M., Namjesnik-Dejanovic, K., Maurice, P.A., Chin, Y.P. and Aiken, G.R. (1999) Fractionation of aquatic natural organic matter upon sorption to goethite and kaolinite. Chemical Geology 157(3-4), 275-284.

Milne, C.J., Kinniburgh, D.G. and Tipping, E. (2001) Generic NICA-Donnan model parameters for proton binding by humic substances. Environmental Science & Technology 35(10), 2049-2059.

Murphy, R.J., Lenhart, J.J. and Honeyman, B.D. (1999) The sorption of thorium (IV) and uranium (VI) to hematite in the presence of natural organic matter. Colloids and Surfaces a-Physicochemical and Engineering Aspects 157(1-3), 47-62.

Ochs, M., Cosovic, B. and Stumm, W. (1994) Coordinative and hydrophobic interaction of humic substances with hydrophilic Al2O3 and hydrophobic mercury surfaces. Geochimica Et Cosmochimica Acta 58(2), 639-650.

Peuravuori, J. and Pihlaja, K. (1997) Molecular size distribution and spectroscopic properties of aquatic humic substances. Analytica Chimica Acta 337(2), 133-149.

Reiller, P., Amekraz, B. and Moulin, C. (2006) Sorption of Aldrich humic acid onto hematite: Insights into fractionation phenomena by electrospray ionization with quadrupole time-of-flight mass spectrometry. Environmental Science & Technology 40(7), 2235-2241.

Reiller, P., Moulin, V., Casanova, F. and Dautel, C. (2002) Retention behaviour of humic substances onto mineral surfaces and consequences upon thorium (IV) mobility: case of iron oxides. Applied Geochemistry 17(12), 1551-1562.

Robertson, A.P. and Leckie, J.O. (1994) Humic substances in the global environment and implication on human health. Senesi, N. and Miano, T.M. (eds), pp. 487-492, Elsevier.

Saito, T., Koopal, L.K., van Riemsdijk, W.H., Nagasaki, S. and Tanaka, S. (2004) Adsorption of humic acid on goethite: Isotherms, charge adjustments, and potential profiles. Langmuir 20(3), 689-700.

Sakuragi, T., Sato, S., Kozaki, T., Mitsugashira, T., Hara, P. and Suzuki, Y. (2004) Am(III) and Eu(III) uptake on hematite in the presence of humic acid. Radiochimica Acta 92(9-11), 697-702.

Schlautman, M.A. and Morgan, J.J. (1994) Adsorption of aquatic humic substances on colloidal-size aluminum-oxide particles - Influence of solution chemistry. Geochimica Et Cosmochimica Acta 58(20), 4293-4303.

Schulthess, C.P. and McCarthy, J.F. (1990) Competitive adsorption of aqueous carbonic and acetic-acids by an Aluminum-oxide. Soil Science Society of America Journal 54(3), 688-694.

Van de Weerd, H., van Riemsdijk, W.H., Leijnse, A., 1999. Modeling the dynamic adsorption

desorption of a NOM mixture: effects of physical and chemical heterogeneity. Environmental Science & Technology 33 (10), 1675-1681.

Vermeer, A.W.P., McCulloch, J.K., Van Riemsdijk, W.H. and Koopal, L.K. (1999) Metal ion adsorption to complexes of humic acid and metal oxides: Deviations from the additivity rule. Environmental Science & Technology 33(21), 3892-3897.

Vermeer, A.W.P., van Riemsdijk, W.H. and Koopal, L.K. (1998) Adsorption of humic acid to mineral particles. 1. Specific and electrostatic interactions. Langmuir 14(10), 2810-2819.

Weishaar, J.L., Aiken, G.R., Bergamaschi, B.A., Fram, M.S., Fujii, R. and Mopper, K. (2003) Evaluation of specific ultraviolet absorbance as an indicator of the chemical composition and reactivity of dissolved organic carbon. Environmental Science & Technology 37(20), 4702-4708.

Weng, L.P., Van Riemsdijk, W.H. and Hiemstra, T. (2007) Adsorption of humic acids onto goethite: Effects of molar mass, pH and ionic strength. Journal of Colloid and Interface Science 314(1), 107-118.

Zhou, Q.H., Maurice, P.A. and Cabaniss, S.E. (2001) Size fractionation upon adsorption of fulvic acid on goethite: Equilibrium and kinetic studies. Geochimica Et Cosmochimica Acta 65(5), 803-812.